Supporting Information

Preparation of single-atom palladium catalysts with high photocatalytic hydrogen production performance by means of photochemical reactions conducted with frozen precursor solutions

Ruiyao Xu, Beibei Xu, Xiaomeng You, Danni Shao, Guoliang Gao, Fangfang Li, Xue-Lu Wang* and Ye-Feng Yao*

[a] *Shanghai Key Laboratory of Magnetic Resonance, School of Physics and Electronic Science, East China Normal University, Shanghai 200241, China.*

**Email: xlwang@phy.ecnu.edu.cn (Xuelu Wang); yfyao@phy.ecnu.edu.cn (Yefeng Yao)*

†*Electronic Supplementary Information (ESI) available. See DOI: 10.1039/x0xx00000x*

This file includes:

1.Materials.

Palladium chloride ($PdCl_2$, 99%,Aladdin),Allylpalladium(II)($[PdCl(C_3H_5)]_2$,chloride dimer,98%,Aladdin),Tetraamminepalladium($H_{12}N_6O_6Pd$,99.99%Aladdin).Triethanolamin

e($C_6H_{15}NO_3$,99.0%,Aladdin).The methanol (CH_3OH, 99.9%) was obtained from Sigma-Aldrich,and deuterium oxide (D_2O, 99.9% atom D,containing 0.05% wt. 3-23 (trimethylsilyl)propionic-2,2,3,3-d4 acid) was obtained from Sigma-Aldrich.

Porous C_3N_4 was prepared by thermal condensation with urea as the precursor and nano-silica gel as the template. 10 g precursor and 1 g nano-silica gel were added into 40 ml ethanol. The suspension was stirred at room temperature for 0.5 h, and then the ethanol was removed by a rotary evaporator. Subsequently, the powder was put into an alumina crucible and transferred to the muffle furnace, then annealed at 550 °C for 3 h with a rate of 5 °C/min. After it cools down naturally, the obtained products were added into 20 ml ammonium fluoride solution with a concentration of 4 mol/L, and the mixed solution was placed on a magnetic stirrer for continuous stirring for 24 h. Then, the suspension was centrifuged and fully wash with deionized water and ethanol. Finally, the samples were heated at 60 °C for 12 h and then labeled as porous C_3N_4.

2.XRD characterizations.

Crystal structure and chemical composition of samples were analyzed by X-ray diffractometer (XRD, Agilent 7890B, Germany Bruker), with copper target as target material, 2θ range of 5°~85° and scanning speed of 10 ° min^{-1}.

3.HAADF-STEM characterizations.

Aberration-corrected high-angle annular dark field-STEM images were acquired using a JEM-ARM200F transmission electron microscope operated at 200 kV.[1]

4.The X-ray absorption near-edge structure spectra.

The extended X-ray absorption fine structure (EXAFS) measurements were carried out on the sample at 21A X-ray nanodiffraction beamline of Taiwan Photon Source (TPS), National Synchrotron Radiation Research Center (NSRRC). This beamline adopted 4-bounce channel-cut Si (111) monochromator for mono-beam X-ray nanodiffraction and X-ray absorption spectroscopy. The end-station equipped with three ionization chambers and Lytle/SDD detector after the focusing position of KB mirror for transmission and

fluorescence mode X-ray absorption spectroscopy. The photon flux on the sample is range from 1x1011~3x109 photon/sec for X-ray energy from 6-27 keV.

5.EXAFS fitting parameters.

The obtained XAFS data was processed in Athena (version 0.9.26) for background, pre-edge line and post-edge line calibrations. Then Fourier transformed fitting was carried out in Artemis (version 0.9.26). The k^2 weighting, k-range of 3 - 13 $Å^{-1}$ and R range of 1 - ~3 Å were used for the fitting of Pd foil; k-range of 3 – 9 $Å^{-1}$ and R range of 1 - ~2.2 Å were used for the fitting of samples. The four parameters, coordination number, bond length, Debye-Waller factor and E_0 shift (CN, R, ΔE_0) were fitted without anyone was fixed, the σ^2 was set.

6.Wavelet Transform parameters.

For Wavelet Transform analysis, the $\chi(k)$ exported from Athena was imported into the Hama Fortran code. The parameters were listed as follow: R range, 1 - 4 Å, k range, 0 - 12 $Å^{-1}$ for samples; k weight, 3; and Morlet function with κ=10, σ=1 was used as the mother wavelet to provide the overall distribution.

7.XPS characterization.

X-ray photoelectron spectroscopy measurements were performed using X-ray photoelectron spectrometer (Escalab 250Xi) equipped with an Al Kα radiation source (1487.6 eV) and hemispherical analyzer with a pass energy of 30.0 eV and an energy step size of 0.05 eV.Spectral deconvolution was performed by Shirley background subtraction using a Voigt function convoluting the Gaussian and Lorentzian functions.

8.FT-IR characterization.

FT-IR (NEXUS 670) was applied to test the functional groups.

9.PL spectra.

The photoluminescence (PL) spectra has been widely used to study the reaction mechanism in the photocatalytic process.

10.UV-vis spectra.

Diffuse reflection spectra (DRS) were performed on the samples using a UV-vis spectrophotometer (3010, Hitachi, Japan), barium sulfate was used as a reference.

11.ICP-MS

The metal loading contents of atomically dispersed metal materials were measured and confirmed by ICP-MS measurements (ELAN DRC-e).[1]

12.AIMD method

All calculations were performed using the plane wave based periodic DFT method as implemented in the Vienna Ab Initio Simulation Package (VASP).[2] The electron-ion interaction was described with the projector augmented wave (PAW) method.[3] The electron exchange and correlation energies were treated within the generalized gradient approximation in the Perdew-Burke-Ernzerhof functional (GGA-PBE).The plane wave basis was set up to 500 eV.

Ab initio molecular dynamics (AIMD) was carried out to obtain configurations.AIMD task was performed over 90000 steps in the NVT ensembles at 200 or 300 K using a small-time step of 0.1 fs due to the lightweight of H+.

13.RDF method

Examining RDF before and after AIMD evolution at elevated temperatures shows that structural ordering or disordering occurs in different phases which can be obtained from the open source software of VMD.

14.Gibbs free energy (ΔG_H) calculation

The barrier (Ea) and reaction energy (Er) are calculated according to Ea = GTS – GFS where GIS, and GFS are the Gibbs free energies of the corresponding states at 300 K, respectively. Gibbs free energies for different adsorption states were calculated as below (here taking OH adsorbing on the substrate for example, named as sub_OH):

G (sub_OH)= H(sub_OH) – T×S(sub_OH)

H(sub_OH) = EDFT(sub_OH) + EZPE(sub_OH) + EH(sub_OH)

Where H(sub_OH) is the thermodynamically corrected enthalpy of sub_OH (eV), S(sub_OH) is the entropy of sub_OH (eV K-1), EDFT(sub_OH) is the static electron energy of sub_OH (eV), EZPE(sub_OH) is the zero point energy of sub_OH (eV), EH(sub_OH) is the enthalpy contribution of sub_OH (eV), and T is the temperature (K).

Photocatalytic decomposition of water for hydrogen production experiment.

The catalyst sample of 20 mg was weighed and put into a quartz reactor. 40 ml of deionized water and 10 ml of triethanolamine (TEOA) were measured and poured into the reactor, TEOA was used as a sacrificial agent. The circulation system was vacuumed to exhaust air, and then the reactor was vacuumed. The entire vacuuming time should exceed 20 mins to fully remove air and make sure that the reaction system is in a vacuum,to prevent other gas components from entering the chromatography and interfering with the experiment. Rely on circulating condensed water, the temperature of the reaction environment was maintained at 6 ℃,to prevent water vapor from entering the chromatography and interfering with the experiment. In order to make the light evenly, use magnetic stirrer to stir the suspension in the process of the whole photocatalytic experiment. GC2060 (Shanghai Ruimin instrument co., LTD., high purity argon as carrier gas) was used for the accurate determination of H_2. The light source is a 300 W Xe lamp(PLS-SXE 300, PerfectLight) with a wavelength range of 400-780 nm.[4]

Photocurrent measurements

Preparation of membrane electrode. 10 mg sample and 2 mg naphthol powder were weighed respectively, and ultrasound was conducted for 30 minutes to make it fully dispersed in 200 μl of Dimethyl formamide (DMF). Then, the dispersed liquid was uniformly coated on the treated conductive indium tin oxide glass (ITO) surface with a pipette gun, and naturally dried for 12 h to obtain a stable membrane electrode.The photoelectric chemistry of the catalyst was tested on a self-assembled system consisting

of a light source (300W Xenon lamp, visible light filter with Vis 420 nm),an electrochemical workstation and an electrolytic cell. The measurement of photoelectric properties was performed in a quartz electrolytic cell with three electrode systems: working electrode, Ag/AgCl electrode worked as reference electrode, platinum wire was used as counter electrode, and the electrolyte was a 0.1mol/L Na_2SO_4 solution. The working electrode is coated with ITO glass sheet of photocatalytic material. Photocurrent test using current-time measurement mode, set bias to 0.5 V.[4]

NMR experiments.

^1H solution nuclear magnetic resonance (NMR) spectra were obtained Varian 700 M spectrometer (16.4T). ^1H NMR experiments were referenced to 3-trimethylsilylpropionic acid (TMSP) and performed at 276 K.[5] The NMR diffusion-order spectroscopy (DOSY) experiments were under 298K and 276K.Data processing of NMR spectra were performed using the Bruker software TopSpin.[6] The prepared samples were irradiated with 300 W Xe lamp under visible light. (Beijing Perfectlight Science and Technology Co., Ltd).

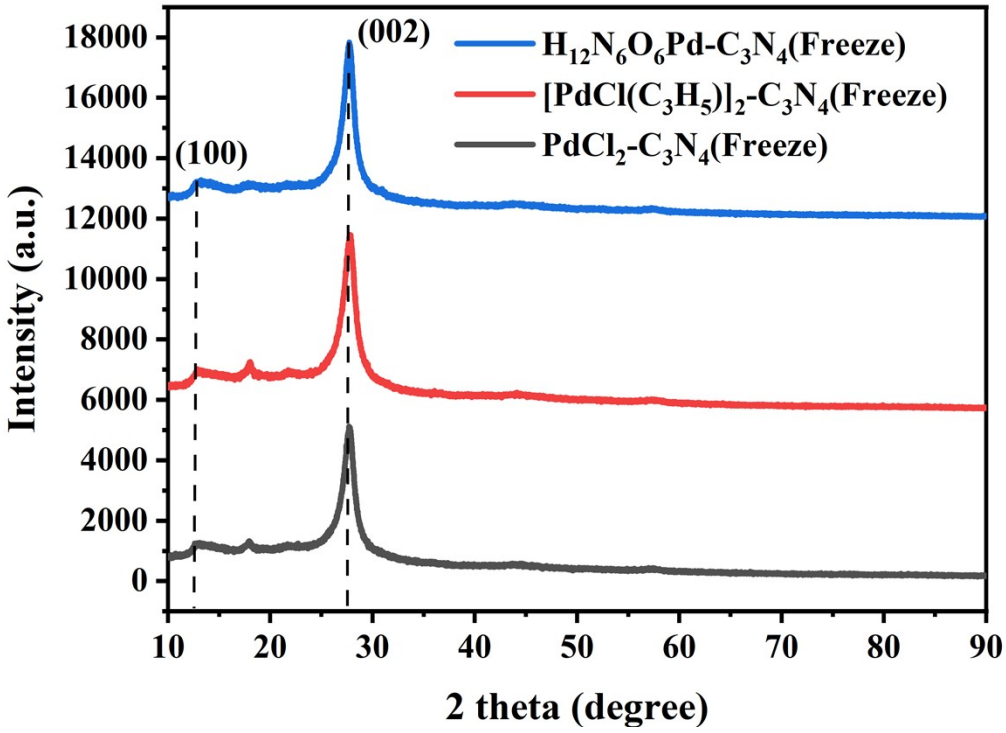

Fig. S1 XRD spectra of the three Pd-C_3N_4 catalysts prepared by iced-photochemical with loading capacity of 0.3wt%.

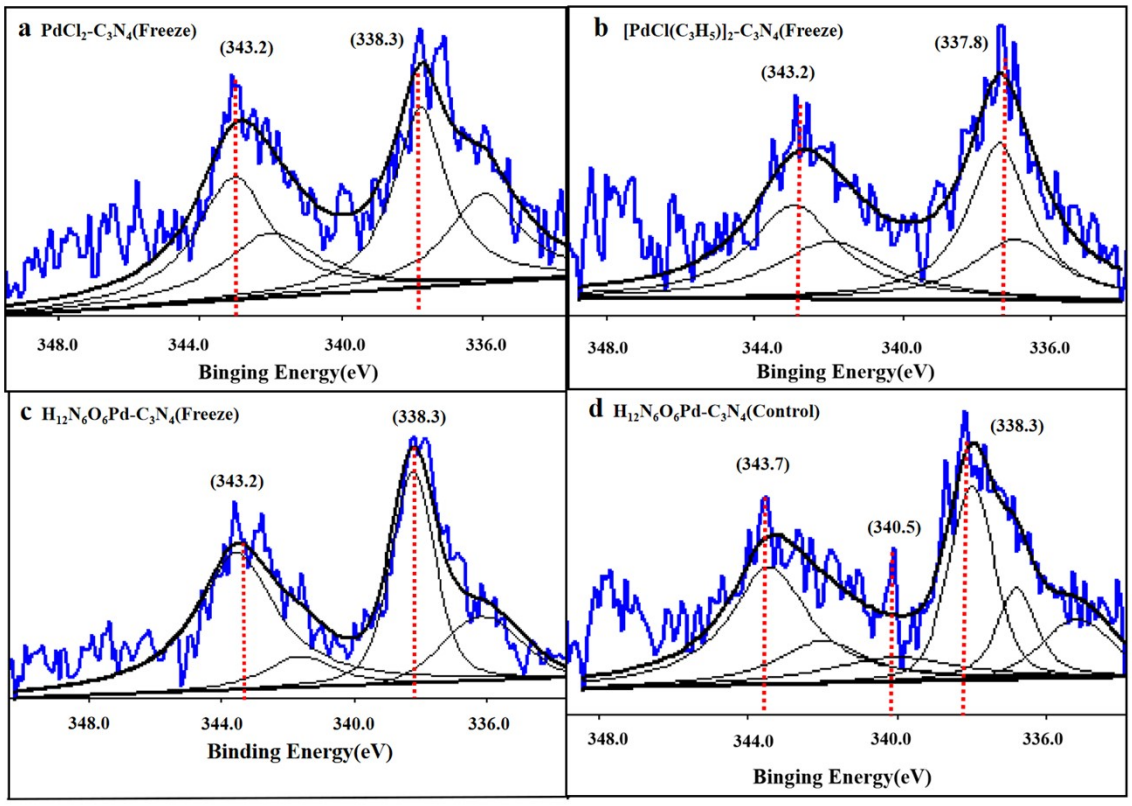

Fig. S2 The XPS spectra of the $PdCl_2$-C_3N_4 (Freeze), $[PdCl(C_3H_5)]_2$-C_3N_4 (Freeze), $H_{12}N_6O_6Pd$-C_3N_4 (Freeze) SACs and $H_{12}N_6O_6Pd$-C_3N_4 (Control).

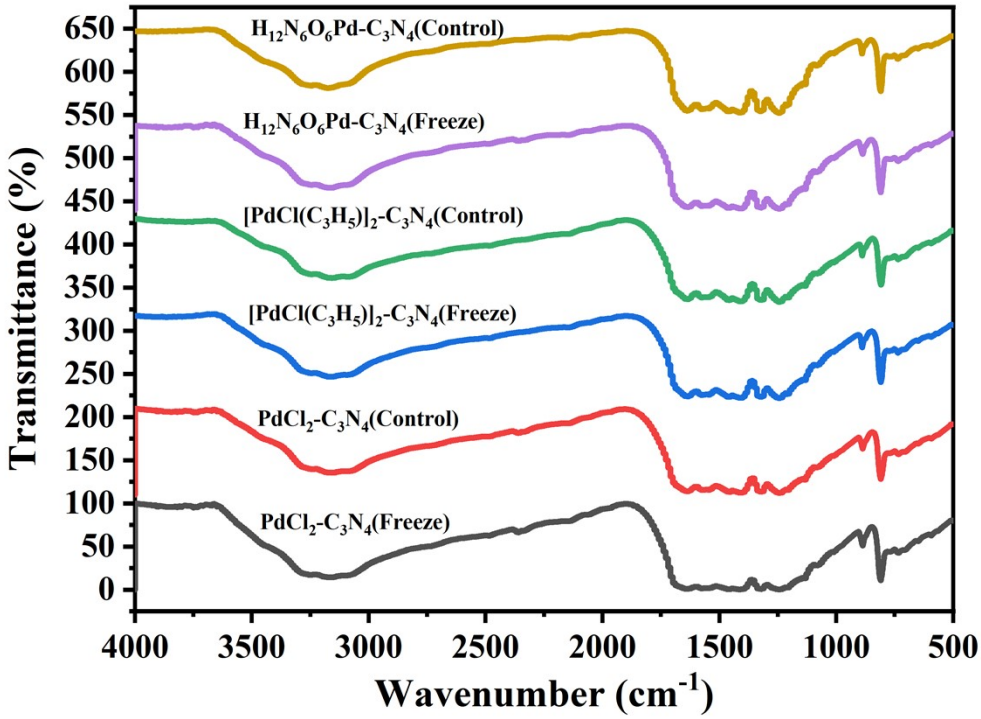

Fig. S3 FT-IR spectra of the Pd-C_3N_4 prepared by iced-photochemical with loading capacity of 0.3wt% and their control groups.

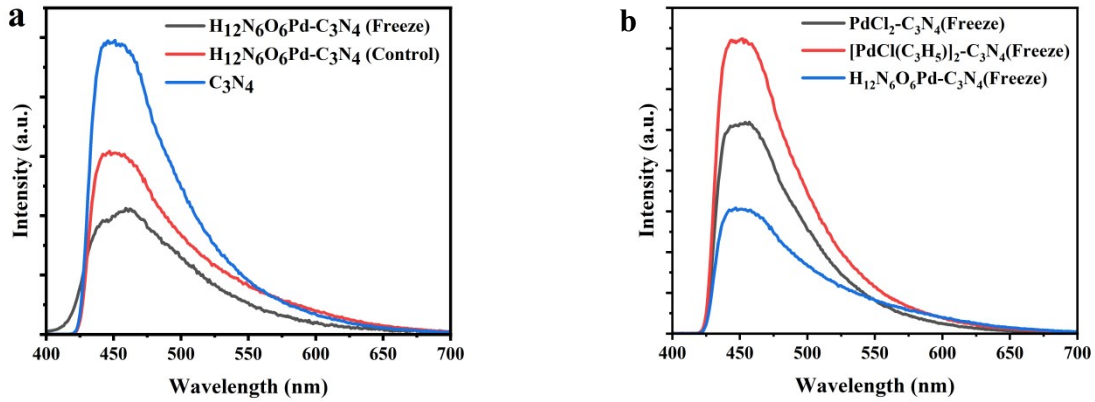

Fig. S4 (a)PL spectra of the $H_{12}N_6O_6Pd$-C_3N_4 (Freeze) and its control group and pure C_3N_4. (b)PL spectra of the Pd-C_3N_4 prepared by iced-photochemical of three precursor solutions with loading capacity of 0.3 wt%.

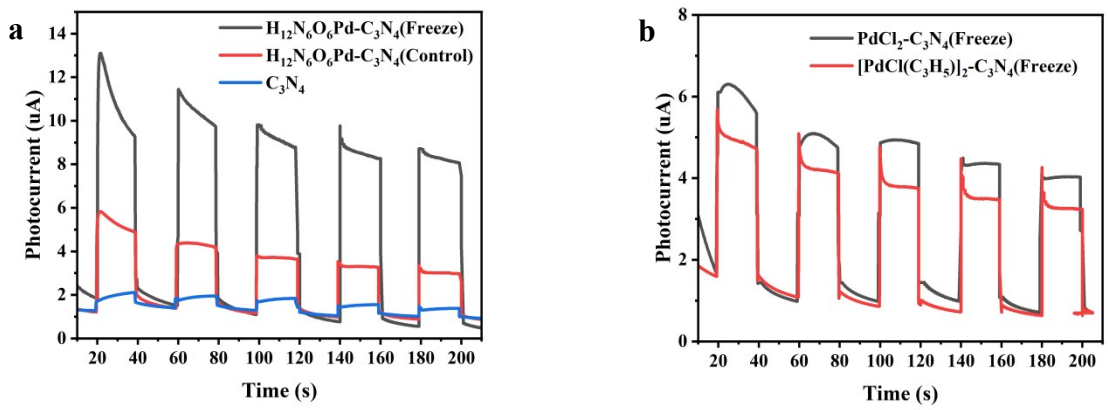

Fig. S5 (a)Transient photocurrent density response of the $H_{12}N_6O_6Pd$-C_3N_4 (Freeze) and its control groups and pure C_3N_4. (b)Transient photocurrent density response of catalysts prepared by iced-photochemical of other two precursor solutions with loading capacity of 0.3 wt%.

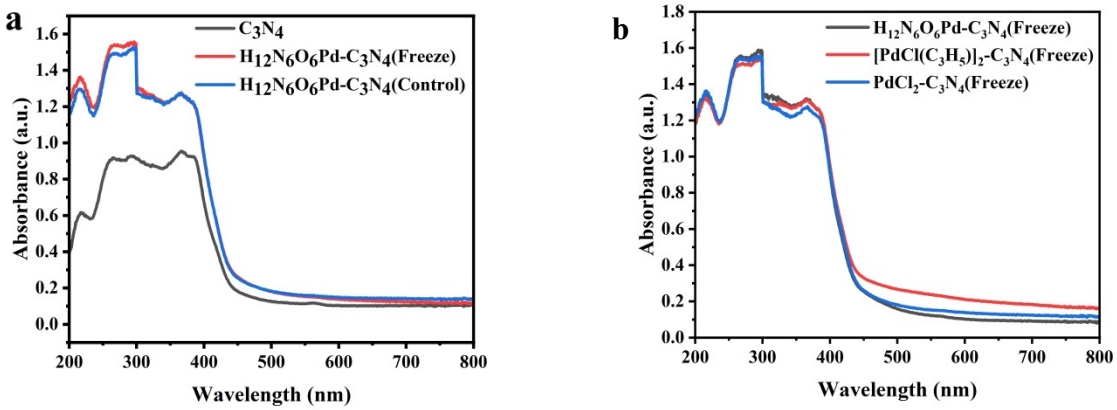

Fig. S6 (a)UV spectra of the $H_{12}N_6O_6Pd$-C_3N_4 (Freeze) and its control group and pure C_3N_4. (b)UV spectra of the Pd-C_3N_4 prepared by iced-photochemical of three precursor solutions with loading capacity of 0.3 wt%.

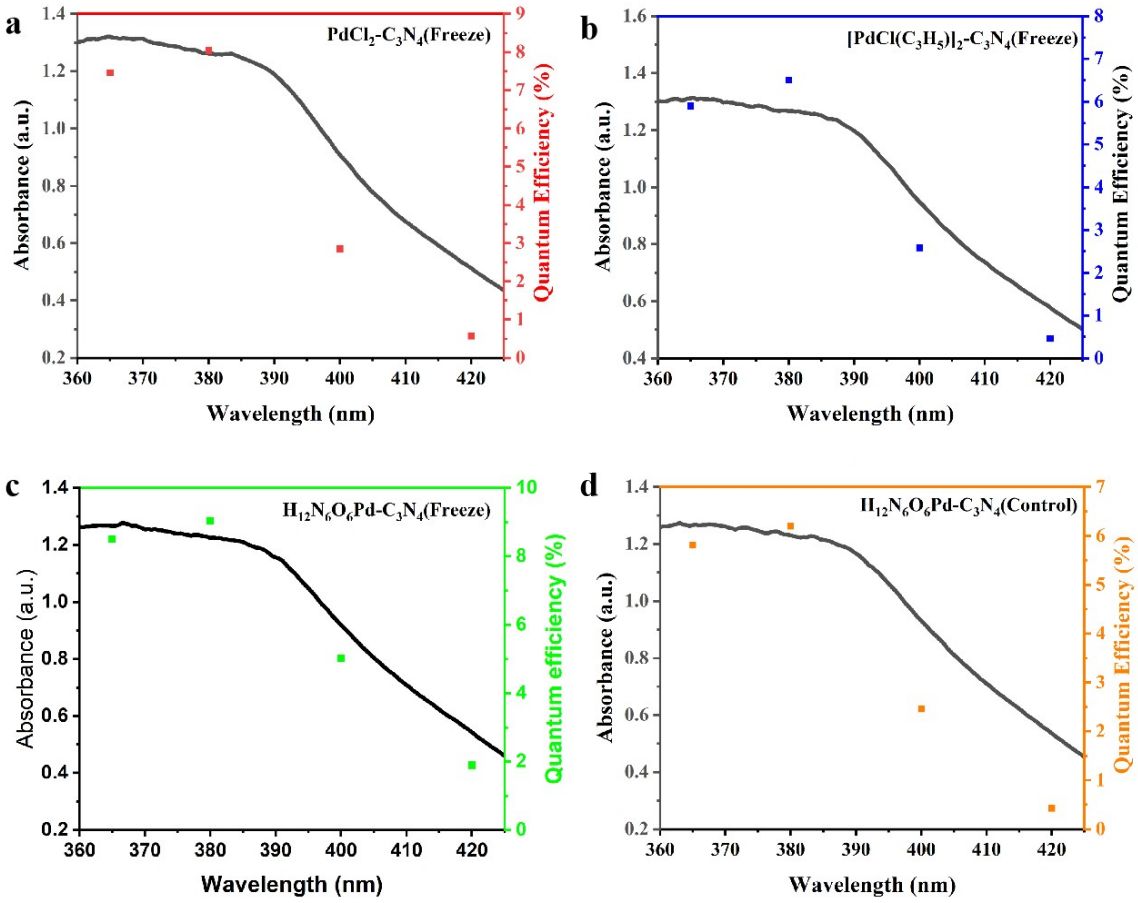

Fig. S7 The quantum efficiency values of the $PdCl_2$-C_3N_4(Freeze), $PdCl(C_3H_5)]_2$-C_3N_4 (Freeze), $H_{12}N_6O_6Pd$-C_3N_4(Freeze) SACs and $H_{12}N_6O_6Pd$-C_3N_4 (Control).

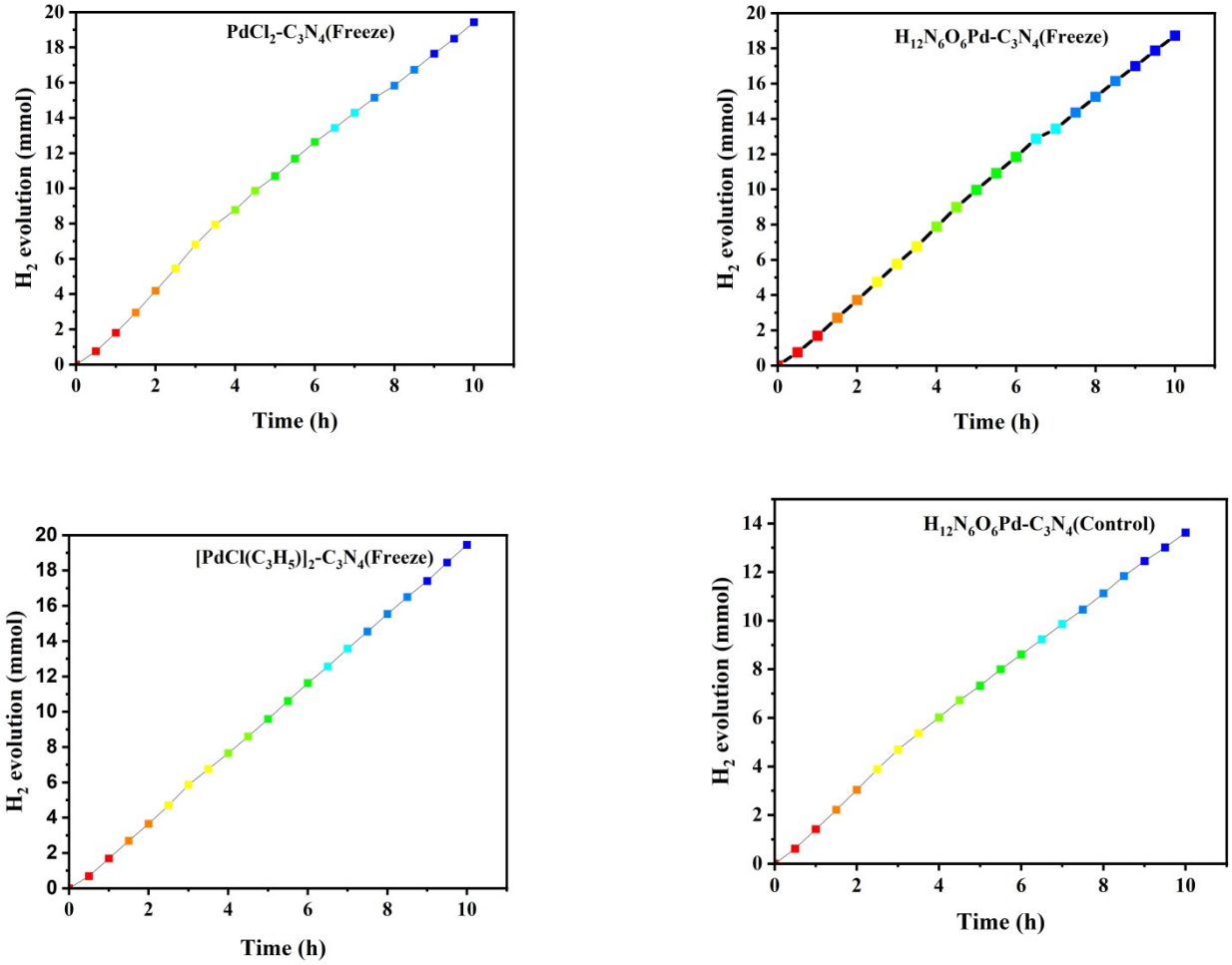

Fig. S8 Photostability study of photocatalytic H_2 evolution over the $PdCl_2$-C_3N_4 (Freeze), $H_{12}N_6O_6Pd$-C_3N_4(Freeze), $[PdCl(C_3H_5)]_2$-C_3N_4(Freeze) and $H_{12}N_6O_6Pd$-C_3N_4 (Control).

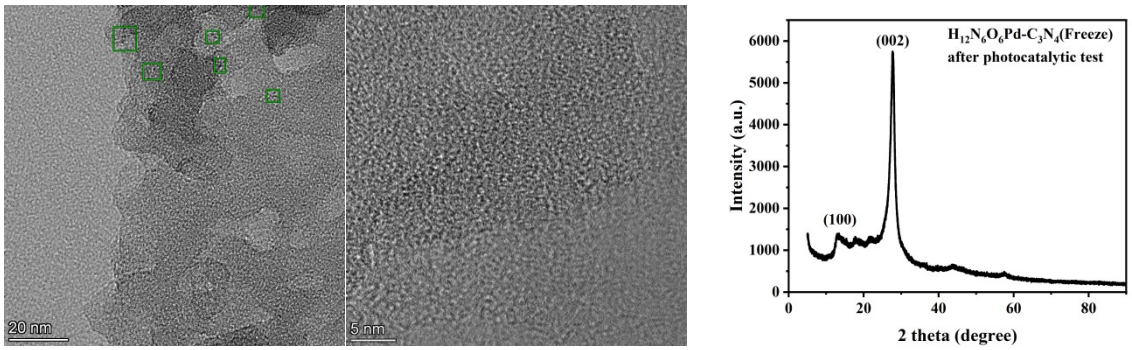

Fig. S9 TEM and XRD spectra of the $H_{12}N_6O_6Pd$-C_3N_4 after photocatalytic tests.

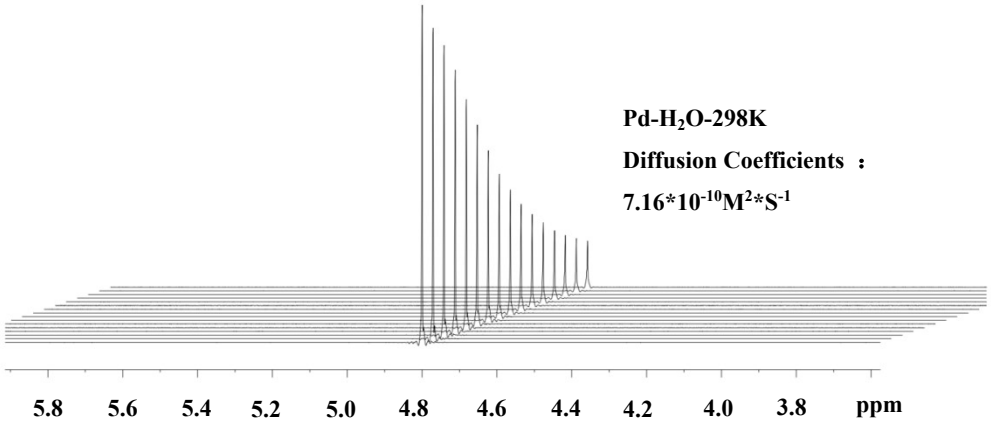
Pd-H2O-298K
Diffusion Coefficients ：
7.16*10-10M2*S-1
5.8
5.6
5.4
5.2
5.0
4.8
4.6
4.4
4.2
4.0
3.8
ppm

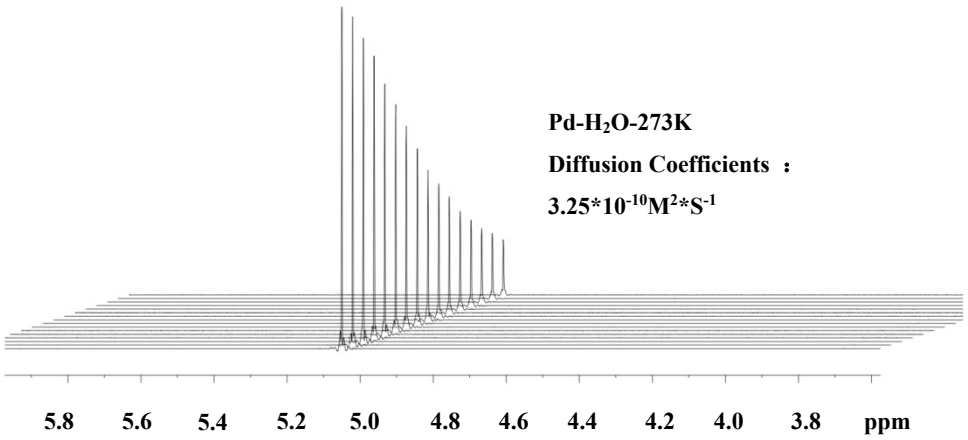
Pd-H2O-273K
Diffusion Coefficients ：
3.25*10-10M2*S-1
5.8
5.6
5.4
5.2
5.0
4.8
4.6
4.4
4.2
4.0
3.8
ppm

Fig. S10 The spectra of the NMR DOSY experiments results.

	shell	CN	R(Å)	σ^2	ΔE_0	R factor
Pd foil	Pd-Pd	12	2.74±0.01	0.0055	3.7±0.4	0.0027
$H_{12}N_6O_6Pd$-C_3N_4(Freeze)	Pd-N	3.4±0.2	2.03±0.01	0.0043	2.9±1.8	0.0063

[a]*N*: coordination numbers; [b]*R*: bond distance; [c]σ^2: Debye-Waller factors; [d] ΔE_0: the inner potential correction. *R* factor: goodness of fit.

Table. S1 EXAFS fitting parameters at the Pd K-edge for various samples(S_0^2=0.83).

Samples	Band gap(eV)
$PdCl_2$-C_3N_4(Freeze)	2.89
$PdCl_2$-C_3N_4(Control)	2.91
$[PdCl(C_3H_5)]_2$-C_3N_4(Freeze)	2.89
$[PdCl(C_3H_5)]_2$-C_3N_4(Control)	2.90
$H_{12}N_6O_6Pd$-C_3N_4(Freeze)	2.88
$H_{12}N_6O_6Pd$-C_3N_4(Control)	2.95

Table. S2 The band gap (Eg) of catalysts prepared by iced-photochemical with loading capacity of 0.3 wt% and their control groups.

Samples	TOF(h^{-1})
$PdCl_2$-C_3N_4(Freeze)	270.3
$PdCl_2$-C_3N_4(Control)	153.5
$[PdCl(C_3H_5)]_2$-C_3N_4(Freeze)	211.4
$[PdCl(C_3H_5)]_2$-C_3N_4(Control)	128.1
$H_{12}N_6O_6Pd$-C_3N_4(Freeze)	309.9
$H_{12}N_6O_6Pd$-C_3N_4(Control)	161.8

Table. S3 The TOFs of catalysts based on Pd.

Samples	Preparation method	H_2 evolution (mmol/g/h)	Ref.
Pd/g-C_3N_4(SAC)	Anchoring Pd atoms onto the g-CN surface	6.688	[7]
Pd/g-C_3N_4(SAC)	Facile liquid-phase adsorption deposition	0.728	[8]
Fe/g-C_3N_4(SAC)	Simultaneous introduction of single-site iron atoms and functionalization of marginal amino groups into the g-C_3N_4 network	3.390	[9]
Au/g-C_3N_4(SAC)	Pretreatment of g-CN with H_2O_2 can introduce active C–OH groups that can react with $HAuCl_4$ to immobilize single atom Au in the g-CN	0.079	[10]

Table. S4 The photocatalytic hydrogen evolution performance of some reported single-atom metal catalysts relevant to this paper.

Samples	Weight(g)	Capacity(wt%)
$PdCl_2$-C_3N_4(Freeze)	0.0332	0.260
$PdCl_2$-C_3N_4(Control)	0.0281	0.253
$[PdCl(C_3H_5)]_2$-C_3N_4(Freeze)	0.0331	0.220
$[PdCl(C_3H_5)]_2$-C_3N_4(Control)	0.0263	0.209
$H_{12}N_6O_6Pd$-C_3N_4(Freeze)	0.0335	0.2855
$H_{12}N_6O_6Pd$-C_3N_4(Control)	0.0316	0.255

Table. S5 ICP-MS of three experimental groups and their control groups.

Reference

1. H. Wei, K. Huang, L. Zhang, B. Ge, D. Wang, J. Lang, J. Ma, D. Wang, S. Zhang and Q. J. A. C. Li, Angew Chem, 2018, 130, 3579-3579.

2. J. Pan, 225th ECS Meeting. 2014.

3. Y. Su, X. Wei, F. Peng, Y. Zhong, Y. Lu, S. Su, T. Xu, S. T. Lee and Y. J. N. L. He, Nano Lett, 2012, 12, 1845-1850.

4. G. L. Gao, ; X. X. Niu,.C. S. T. Catal Sci Technol, 2020, 10.

5. M. Ye, B.-B. Xu, R. Zhang, Y.-N. Yang, L.-Y. Yang, X. L. Wang and Y.-F. J. J. o. C. Yao, J. Catal, 2019, 378, 36-41.

6. B.-B. Xu, M. Zhou, M. Ye, L.-Y. Yang, H.-F. Wang, X. L. Wang and Y.-F. J. J. o. t. A. C. S. Yao,J. Am. Chem. Soc, 2021, 143, 10940-10947.

7. S. Cao, H. Li, T. Tong, H. C. Chen, A. Yu, J. Yu and H. M. J. A. F. M. Chen. Adv Funct Mater, 2018, 28, 1802169.

8. L. Liu, X. Wu, L. Wang, X. Xu, L. Gan, Z. Si, J. Li, Q. Zhang, Y. Liu and Y. J. C. C. Zhao. Commun Chem,2019, 2, 1-8.

9. W Zhang, Q Peng, L Shi, Q Yao, et al. Small, 2019;15:e1905166.

10. L. Zeng, C. Dai, B. Liu and C. J. J. o. M. C. A. Xue.J Mater Chem, 2019, 7.